

# Valley dynamics of different excitonic states in monolayer WSe<sub>2</sub> grown by molecular beam epitaxy

Shengmin Hu<sup>1,2</sup>, Jialiang Ye<sup>1,2</sup>, Ruiqi Liu<sup>1,2</sup>, and Xinhui Zhang<sup>1,2,†</sup>

<sup>1</sup>State Key Laboratory of Superlattices and Microstructures, Institute of Semiconductors, Chinese Academy of Sciences, Beijing 100083, China

<sup>2</sup>College of Materials Science and Opto-electronic Technology, University of Chinese Academy of Sciences, Beijing 100049, China

**Abstract:** Monolayer transition-metal dichalcogenides possess rich excitonic physics and unique valley-contrasting optical selection rule, and offer a great platform for long spin/valley lifetime engineering and the associated spin/valleytronics exploration. Using two-color time-resolved Kerr rotation and time-resolved reflectivity spectroscopy, we investigate the spin/valley dynamics of different excitonic states in monolayer WSe<sub>2</sub> grown by molecular beam epitaxy. With fine tuning of the photon energy of both pump and probe beams, the valley relaxation process for the neutral excitons and trions is found to be remarkably different—their characteristic spin/valley lifetimes vary from picoseconds to nanoseconds, respectively. The observed long trion spin lifetime of > 2.0 ns is discussed to be associated with the dark trion states, which is evidenced by the photon-energy dependent valley polarization relaxation. Our results also reveal that valley depolarization for these different excitonic states is intimately connected with the strong Coulomb interaction when the optical excitation energy is above the exciton resonance.

**Key words:** TMDCs; excitons; valley polarization lifetime; two-color time-resolved Kerr rotation spectroscopy

**Citation:** S M Hu, J L Ye, R Q Liu, and X H Zhang, Valley dynamics of different excitonic states in monolayer WSe<sub>2</sub> grown by molecular beam epitaxy[J]. *J. Semicond.*, 2022, 43(8), 082001. <https://doi.org/10.1088/1674-4926/43/8/082001>

## 1. Introduction

The monolayers of the transition metal dichalcogenides (TMDCs), such as MoS<sub>2</sub> and WSe<sub>2</sub>, are direct bandgap semiconductors with two inequivalent valleys at the corners of the hexagonal Brillouin zone. Owing to the inversion symmetry breaking and strong spin-orbit interactions, the interband transition determined by the valley-contrasting optical selection rule can give rise to a generation of valley pseudospin in TMDC monolayers<sup>[1–3]</sup>. Thus, the valley polarization of TMDC monolayers can be optically generated and detected through optical excitation with the selective helicity<sup>[4–12]</sup>. The time-resolved photoluminescence (TRPL), time-resolved Kerr rotation (TRKR) or Faraday rotation spectroscopy have been utilized to explore the intrinsic spin/valley lifetime and the physical origin of depolarization<sup>[13–20]</sup>. Interestingly, the measured time constants of the Kerr or Faraday signals in monolayer WSe<sub>2</sub> differ by more than three orders of magnitude from a few picoseconds to tens of nanoseconds, largely depending on the prepared monolayers and experimental conditions. The observed long-lived spin relaxation process near the trion resonance on the time scale of nanoseconds or even longer for WSe<sub>2</sub> is proposed to be associated with either a transfer from trion's spin polarization to the resident electrons/holes<sup>[16, 18, 19]</sup> or the inherent feature of trion itself<sup>[20–22]</sup>. Although the nature of the observed long trion spin lifetime remains an issue of debate, these studies illustrate the feasibility of the long lifetime of valley pseudospin in monolayer TMDCs favorable for future application in valleytronics.

It is known that the monolayer WSe<sub>2</sub> exhibits strong and rich excitonic effects. The neutral excitons and trions, as well as other Coulomb-correlated complexes such as the localized excitons, biexcitons and dark excitons in the mechanically exfoliated WSe<sub>2</sub> monolayers, have been investigated previously<sup>[23–30]</sup>. It is thus a good material platform to explore the valley dynamics of different excitonic states and the associated physical mechanisms, which is fundamentally important for the spin/valleytronics application based on TMDCs materials. However, the spin/valley polarization dynamics in WSe<sub>2</sub> monolayer grown by molecular beam epitaxy (MBE) is rarely reported at present. Compared with the mechanically exfoliated and CVD-grown monolayer TMDCs, MBE-grown TMDCs monolayers are expected to exhibit improved quality with fewer interfacial defects and less disorder, and thus provide an alternative approach for achieving novel opto- and spin-electronic devices based on large-area TMDCs.

In this work, we present a systematic study of the valley polarization dynamics of the neutral excitons and trions in MBE-WSe<sub>2</sub> monolayer grown on a sapphire substrate by using the ultrafast two-color TRKR spectroscopy. Thanks to the continuous tunability and flexible selection of the excitation laser wavelength, as well as the sub-picosecond time resolution with a similar method as in our previous work<sup>[31]</sup>, valley polarization relaxation processes of the neutral excitons and trions are investigated by selectively tuning both the pump and probe photon energy, and the remarkable difference in valley lifetime for these excitonic states is uncovered. In contrast to the much shorter valley polarization lifetime for the neutral excitons (~1.5 ps), the valley polarization lifetime of trion was found to be ~2.4 ns. With a remarkable valley spin lifetime change observed for trion by a systematical tuning of pump/probe photon energy, it was concluded that the long

Correspondence to: X H Zhang, [xinhuiz@semi.ac.cn](mailto:xinhuiz@semi.ac.cn)

Received 27 JANUARY 2022; Revised 9 MARCH 2022.

©2022 Chinese Institute of Electronics

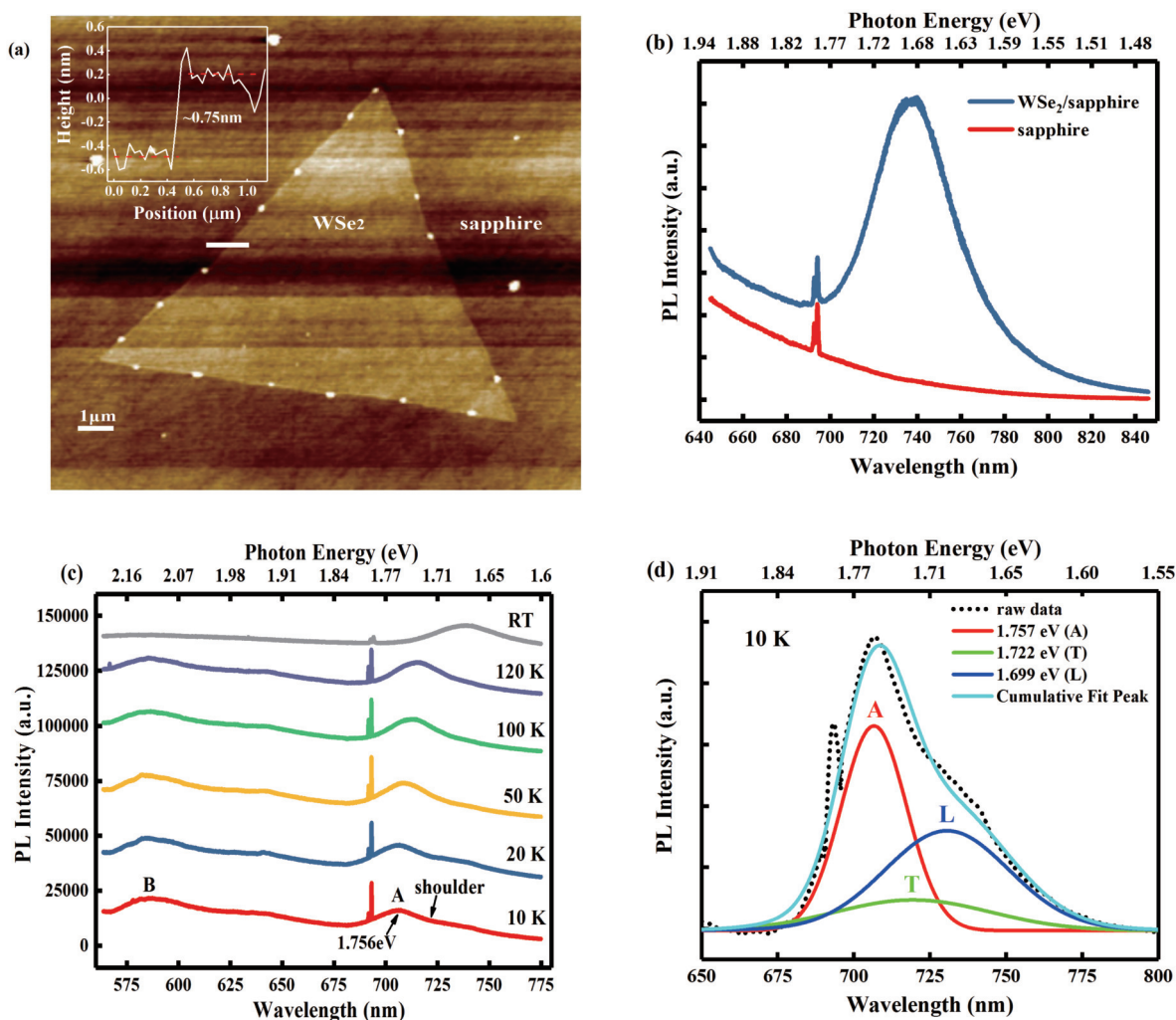


Fig. 1. (Color online) (a) AFM micrograph of the monolayer  $\text{WSe}_2$  grown on sapphire substrate, the inset is the height profile of the monolayer MBE- $\text{WSe}_2$ . (b) Room temperature PL spectra of the as-grown monolayer  $\text{WSe}_2$  on sapphire and sapphire substrate itself. (c) The PL spectra of MBE- $\text{WSe}_2$  monolayer as a function of temperature. (d) PL spectrum and Gaussian fit of MBE- $\text{WSe}_2$  monolayer measured at 10 K.

valley spin lifetime change for trion was associated with the formation of dark trions by intervalley scattering process.

## 2. Experimental details

For both the time-resolved reflectivity (TRR) and TRKR experiments, we used a mode-locked femtosecond Ti:sapphire laser (Chameleon Ultra II, Coherent, Inc.) that was equipped with an optical parameter oscillator (OPO) to independently tune the photon energies of both pump and probe pulses. Further fine tuning of probe energy was accomplished by choosing ultra-narrow pulses with band-pass filters from a super-continuum white light, which was generated by a nonlinear photonic crystal fiber (FemotoWHITE-800, NKT Photonics) under excitation of the Ti:sapphire laser. The temporal pulse width is about 150 fs for both the pump and probe pulses. The time-averaged powers for the pump and probe beam are set to be 700 and 70  $\mu\text{W}$ , respectively, with a spot diameter of about 2  $\mu\text{m}$ . A detailed scheme of the experimental setup can be found in Ref. [31, 32]. For the TRR measurement, both the pump and probe pulses are linearly polarized, with the reflected probe beam detected by a silicon photodetector. Whereas for the TRKR measurement, the pump pulse is set to be circularly polarized and the reflected probe beam is detected by a silicon balanced photodetector in combination with

a Wollaston prism and a half waveplate to achieve a sensitive detection of the weak Kerr rotation signal. The investigated  $\text{WSe}_2$  monolayer was grown on a sapphire substrate by molecular beam epitaxy (2D Semiconductors, Inc.).

## 3. Results and discussions

The studied monolayer MBE- $\text{WSe}_2$  grown on sapphire was first characterized by atomic force microscope (AFM), as shown in Fig. 1(a). The height profile in the inset confirmed that the thickness of  $\text{WSe}_2$  is about 0.75 nm, corresponding to a monolayer. Then, the photoluminescence (PL) of MBE- $\text{WSe}_2$  monolayer and its sapphire substrate at room temperature was investigated by using a 532 nm continuous-wave laser excitation, the results are shown in Fig. 1(b). A strong PL peak at 740 nm (1.675 eV) at room temperature, which corresponds to A exciton of monolayer  $\text{WSe}_2$ [13, 16, 33, 34], again confirms the monolayer nature of the studied MBE- $\text{WSe}_2$  on sapphire substrate. In addition, a sharp PL peak can be observed at 1.789 eV for both  $\text{WSe}_2$  monolayer and its sapphire substrate. The PL response at 1.789 eV coincides with the fluorescence position of chromium ions[35]. This implies that chromium ions are present in the sapphire substrate, for which the chromium ions were unintentionally doped during the

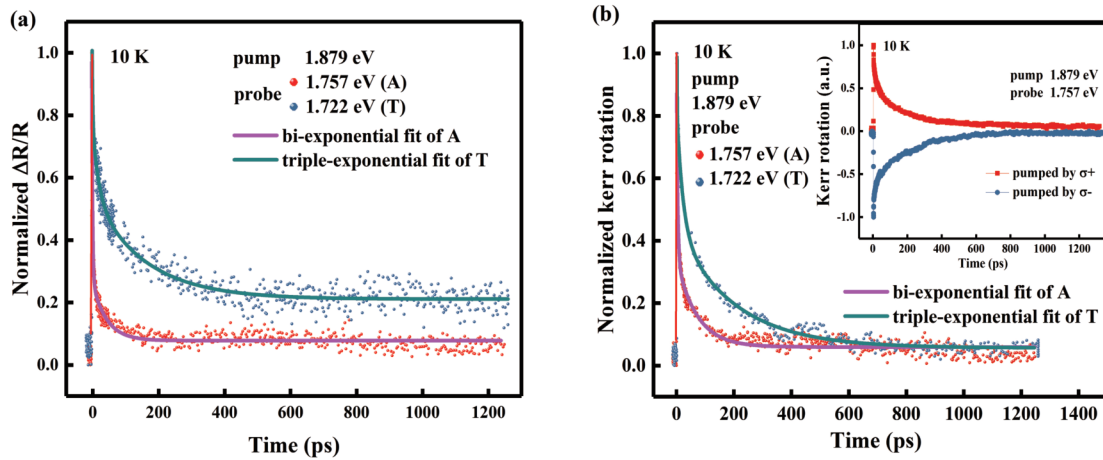


Fig. 2. (Color online) (a) Normalized transient differential reflectivity ( $\Delta R/R$ ) and (b) TRKR signals, with respect to the peak values measured at various probe energies in resonance with A exciton (A) and trion (T), respectively, for MBE-WSe<sub>2</sub> monolayer. Here pump energies are all set at 1.879 eV, and the measured temperature is 10 K. The inset in (b) shows the normalized TRKR response measured under excitation of right- ( $\sigma^+$ , red trace) and left- ( $\sigma^-$ , blue trace) circularly polarized pump beam, with the probe energy to be resonant with A exciton.

growth. This characteristic fluorescence peak can be filtered out through a long-pass filter when studying the valley polarization dynamics of MBE-WSe<sub>2</sub> monolayer. Then, the PL spectra of MBE-WSe<sub>2</sub> monolayer at different temperatures were measured as shown in Fig. 1(c). The obvious PL peaks at 1.757 and 2.110 eV at 10 K are assigned to be the A and B excitons of WSe<sub>2</sub>, according to previously reported results<sup>[33, 34]</sup>. It is also observed that the PL peak of A exciton for MBE-WSe<sub>2</sub> monolayer exhibits a redshift of approximately 40 meV compared with the mechanically exfoliated monolayer WSe<sub>2</sub> on a Si/SiO<sub>2</sub> substrate. According to previous studies, this redshift may result from a different dielectric environment or interfacial strain<sup>[36, 37]</sup>. The PL peak of A exciton shows significant redshifts with increasing temperature (as expected), while the PL peak of B exciton shows slight blueshifts, first at low temperature and then redshifts at higher temperature, which may result from the thermal activation of the trapped excitons. This suggests that there may be unintentional shallow defects states slightly below the conduction band, so that the B excitons involving the lowest conduction band tend to be trapped more easily than A excitons. With the increase of temperature, the trapped excitons can be thermally activated into the delocalized states and captured by the competing nonradiative decay channels or recombine as free excitons, giving rise to slight blueshifts of B exciton with the carrier redistribution in band tails<sup>[38, 39]</sup>. Moreover, unlike the mechanically exfoliated monolayer WSe<sub>2</sub>, the A exciton (A), trions (T) and localized excitons (L) cannot be well resolved for MBE-WSe<sub>2</sub>. As seen in Fig. 1(c), one can observe a broad shoulder at low-energy side along with the A exciton. Thus, the PL peaks associated with different excitons were clarified using Gaussian peak fitting, as shown in Fig. 1(d). The three peaks centered at 1.757, 1.722 and 1.699 eV refer to the A exciton, trions and localized excitons, respectively. The trion is peaked approximately 30 meV lower than that of A exciton, so the sample is considered to be n-type doped based on previous studies for WSe<sub>2</sub><sup>[16, 40, 41]</sup>. The full width at half maxima (FWHM) of the A, T, and L peak is 25, 64, 46 nm, respectively. Compared with mechanically exfoliated WSe<sub>2</sub>, the broader peaks may result from defects in MBE-WSe<sub>2</sub>. Moreover, the

much weaker PL of trion than that of A exciton indicates that the density of bright trions is quite low, which also implies that the resident carrier concentration is low in the n-type MBE-grown WSe<sub>2</sub> studied in this work. In addition, the stronger PL of localized excitons infers existence of a substantial number of defect states and disorder in MBE-grown WSe<sub>2</sub>.

The TRR of these excitonic states is then studied first at low temperature of 10 K with a fixed optical pumping wavelength of 660 nm (120 meV above the A exciton) but with different probe photon energies tuned in resonance with A exciton and trions, respectively, as shown in Fig. 2(a). The rising time of all  $\Delta R/R$  signals is limited only by the time resolution of the pump pulse, representing an ultrafast exciton and trion formation time<sup>[42, 43]</sup>. The TRR measurements show multiexponential decay at both probe photon energies resonant with A exciton and trion. The deduced decay time constants at 10 K are 2.4 ps ( $\tau_1$ ) and 43 ps ( $\tau_2$ ) when probing resonantly at A exciton. The fast decay of A exciton is consistent with previous reports for the mechanically exfoliated monolayer WSe<sub>2</sub>, and is related to phonon scattering, trapping, and exciton recombination<sup>[7, 9, 10, 44]</sup>. When probing resonantly at trion, the decay curve can be fitted by a triple exponential decay function, and the respective decay constants of 2.0 ps ( $\tau_1$ ), 20 ps ( $\tau_2$ ), and 159 ps ( $\tau_3$ ) are derived. Direct comparison of the TRR results for A exciton and trion shows a similar decay time scale of  $\tau_1$  and  $\tau_2$  but a much larger spectral weight of the long-lived (>100 ps) decay component for trion. This indicates that trion has different relaxation channels from the A exciton. The similar results in previous reports suggest that the longer decay time  $\tau_3$  of trions may result from the formation of dark trion states<sup>[11, 25, 45]</sup>.

We then studied the TRKR response by turning the linearly polarized pump pulse to a circularly-polarized pump pulse, while the other conditions remained to be the same. The inset of Fig. 2(b) shows the normalized TRKR response of monolayer MBE-WSe<sub>2</sub> with respect to its peak values measured at 10 K with the probe energy resonant with the A exciton. When reversing the helicity of the pump pulse, a reversal sign of the Kerr signal is observed, indicating that the

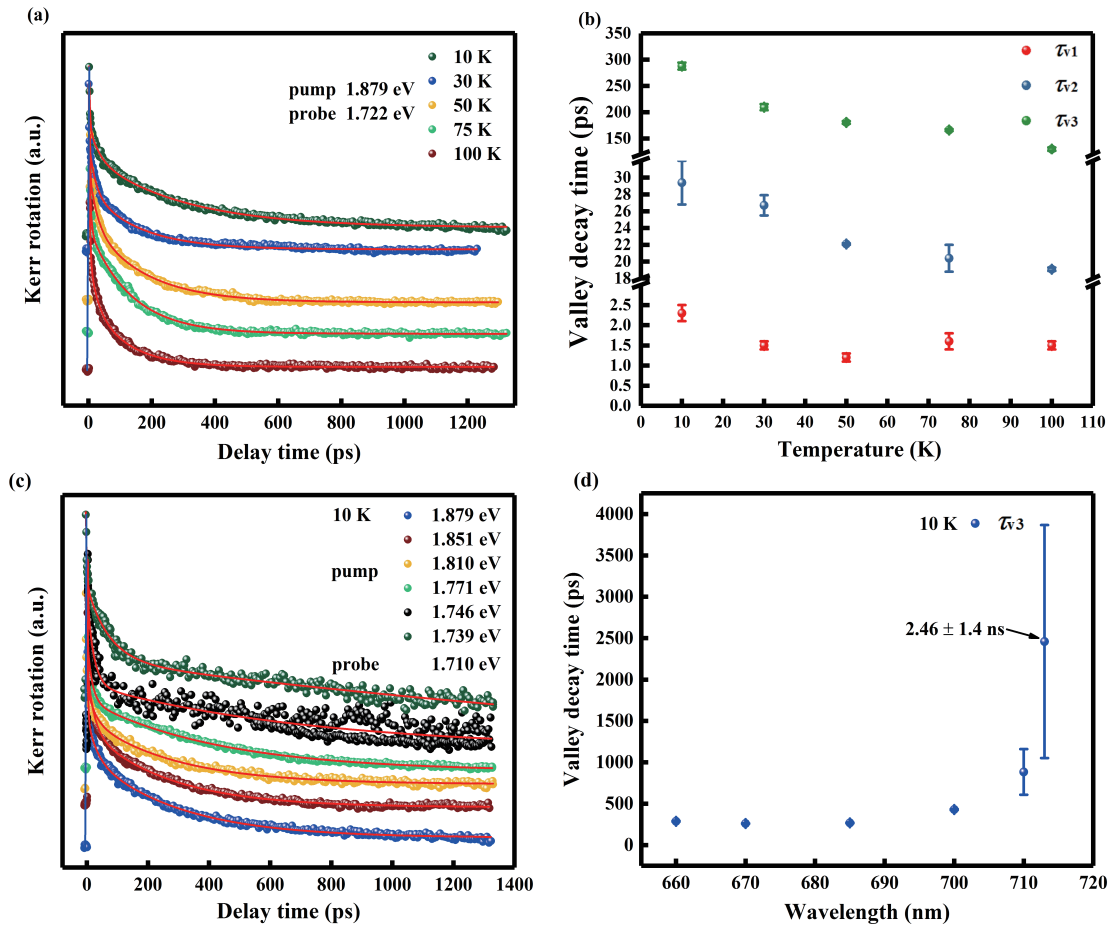


Fig. 3. (Color online) (a) Temperature-dependent TRKR responses and their fittings (solid lines) probed for trion, pump and probe photon energies are set to be 1.879 and 1.722 eV, respectively. (b) Temperature-dependent valley relaxation time deduced from results in (a). (c) TRKR measured at various pump energies with a fixed probe energy of 1.710 eV at 10 K. The solid lines are fitting results. (d) The extracted long valley lifetime  $\tau_{v3}$  as a function of pump wavelength at 10 K.

Kerr signal originates from the optically initialized valley polarization. Upon excitation by the circularly polarized pump pulse, the TRKR signal reaches to the maximum value at a time delay of  $\sim 1$  ps. This suggests that the initially photogenerated excitons are completely polarized in one valley. The temporal decay of the Kerr signal thus reflects the dynamic valley depolarization of A exciton. The Kerr trace of the A exciton is fitted by an exponential decay function with the deduced lifetime  $\tau_{v1} = 3.7 \pm 0.2$  ps, which is on the same order of magnitude as previously reported results for the mechanically exfoliated WSe<sub>2</sub>[13, 31]. This fast exciton valley depolarization is well known to result from mainly the electron-hole Coulomb exchange interaction[46]. Note that the depolarization at near-resonant excitation can be different from that of on-resonant excitation because the efficiency of this exchange mechanism depends on the center-of-mass momentum of excitons[47].

When probing resonantly at trion, the TRKR signal first exhibits a fast drop from the initial value, followed by a long-lived decay tail, as shown in Fig. 2(b). The decay trace probed for trion shown in Fig. 2(b) exhibits a triple-exponential decay behavior with three characteristic time constants:  $2.3 \pm 0.2$  ps ( $\tau_{v1}$ ),  $29.4 \pm 2.6$  ps ( $\tau_{v2}$ ), and  $287.8 \pm 6.6$  ps ( $\tau_{v3}$ ). Thus, the trion of MBE-WSe<sub>2</sub> again exhibits longer valley lifetime compared to the A exciton even under non-resonant excitation, as has been reported previously for the mechanically exfo-

liated monolayer WSe<sub>2</sub>. It is noted that the first decay constant of trion is roughly the same as the valley polarization lifetime of the measured A exciton. Previous ultrafast time- and valley-resolved measurements have unraveled the valley-dependent many-body processes, including phase space filling and band-gap renormalization effects[8, 48–51]. The absorption bleaching of the trion transition due to the greatly pumped excitons has already been observed[20, 52]. The creation of valley-polarized excitons blocks the trion transition in the same valley owing to the same ground state. These facts suggest that the measured valley depolarization probed at trion's resonance arises from the rapid exciton valley depolarization. This kind of exciton-trion correlation is expected to disappear owing to the largely reduced exciton density when tuning the pump energy far below the A resonance, and this is evidenced as stated below.

To further explore the origination of the observed long valley lifetime of trion, a detailed TRKR investigation of trion by varying temperature and pump photon energy is performed. Fig. 3(a) shows a systematic temperature-dependent TRKR of trion from 10 to 100 K, with pump and probe photon energies of 1.879 and 1.722 eV, respectively. For temperatures higher than 100 K, the signal-to-noise ratio is too small to obtain reliable data. A general trend shows that the valley relaxation time decreases with increasing temperature, indicating an enhanced valley relaxation at higher temperatures.



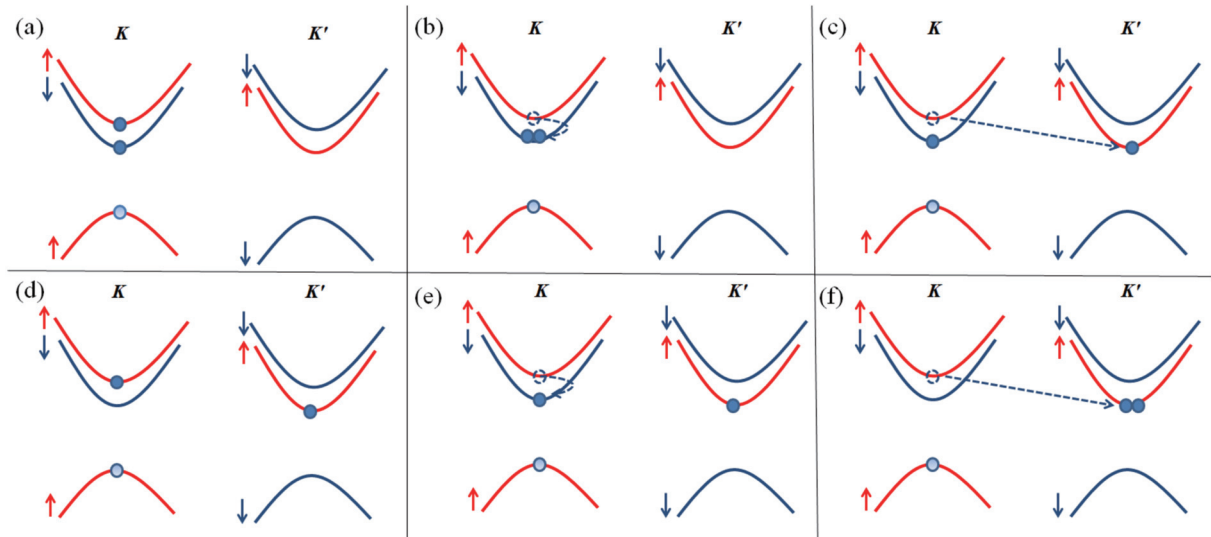


Fig. 4. (Color online) Schematics of the bright and dark trion states in  $\text{WSe}_2$ . (a) A bright singlet trion and (d) a bright triplet trion; when optically excited in the  $K$  valley of  $n$ -doped  $\text{WSe}_2$ . (b), (c), (e), and (f) illustrate the possible conversion channels from bright to dark trions under phonon- or defect-assisted scattering.

Again, one can notice that the fastest decay constant ( $\tau_{v1}$ ) remains at the same magnitude as that of excitons in the entire measurement temperature range. This suggests that this fast process is indeed related to the strong exciton-trion coherent coupling, through which the neutral excitons act as an efficient valley relaxation channel for trions<sup>[52]</sup>.

The intermediate decay time ( $\tau_{v2}$ ), which is within tens of ps, is similar to the emission time of excitons and trions observed in previous TRPL measurements<sup>[11, 23, 39]</sup>. One may speculate that this decay process is related to the photoexcited excitonic radiative recombination, as Kerr rotation actually measures the density of polarized excitons or trions within the probe beam spot area. However, the interband radiative recombination in both valleys is excluded because  $\tau_{v2}$  is observed to decrease with increasing temperature, which contrasts with the increased exciton radiative lifetime at higher temperature expected for the two-dimensional semiconductors<sup>[53, 54]</sup>. According to the broad PL feature for both A and B excitons in Fig. 1(a), there could exist a massive amount of defect states and disorder in MBE-grown  $\text{WSe}_2$ . Thus, the trion valley relaxation channel characterized by  $\tau_{v2}$  may be associated with the defect-assisted recombination, in which the photoexcited electrons are captured easily by the defect levels following fast intervalley scattering and then recombine radiatively<sup>[16]</sup>. In fact, the fine structure of bright trion is also expected to influence the trion valley polarization dynamics, which has been reported for monolayer  $\text{WS}_2$ <sup>[17]</sup> and  $\text{WSe}_2$ <sup>[20]</sup>. It has been demonstrated that the optically bright trions can be formed with an additional carrier located either within the same valley (singlet trions) or in a different valley (triplet trions), and there is an energetic splitting of about 7 meV (trion fine structure) between these states due to the exchange interaction<sup>[21, 55]</sup>. Valley polarization of bright singlet or triplet trions can exhibit fast depolarization within a few ps or tens of ps<sup>[20, 56]</sup>.

The measured long valley lifetime ( $\tau_{v3}$ ) on the order of hundreds of ps, is again comparable to the extracted decay time constant  $\tau_3$  of trions by TRR measurements, as shown in Fig. 2(a). It is thus speculated that the long trion valley life-

time  $\tau_{v3}$  could be related to the spin/valley-polarized intervalley dark trions because there is no obvious difference between the valley lifetime  $\tau_{v3}$  and lifetime of trion itself<sup>[21]</sup>. The previously reported correlation between the TRKR and PL intensity occurring at the trion resonance<sup>[22]</sup> also suggests the conversion of valley-polarized bright trion to the nonradiative dark trion states, in which the intervalley scattering facilitated by either defects or phonons plays an important role<sup>[21, 57]</sup>. With increasing temperature, the valley depolarization process will be enhanced with a shorter  $\tau_{v3}$  because phonons become more active at higher temperature, which is coincident with the observed temperature-dependent trend of  $\tau_{v3}$  shown in Fig. 3(b).

Furthermore, we carefully tune the pump energy below the A exciton resonance, to approach closer to the trion resonance. The TRKR results at 10 K are presented in Fig. 3(c), the valley polarization is observed to persist much longer as the pump energy approaches the T resonance. When slightly reducing the pump energy from 1.771 to 1.739 eV, the valley lifetime for trion exhibits a remarkable change from  $\sim 0.28$  to  $\sim 2.46$  ns correspondingly, as shown in Fig. 3(d). Meanwhile, the spectra weight of this long-lived component appears to significantly decrease, resulting in a larger error bar of valley polarization lifetime  $\tau_{v3}$ . This remarkably different  $\tau_{v3}$  by slight variation of pump photon energy strongly suggests that the observed long valley polarization lifetime is associated with the dark trion, as we speculated earlier. If the long trion valley lifetime is associated with the resident carriers after trion recombination, as proposed in previous study<sup>[15]</sup>, then there would be no such sensitive dependence on the pump photon energy. When the pump energy is tuned to be lower than the A exciton resonance, the exciton formation will be greatly suppressed and the intervalley electron-hole exchange interaction cannot occur effectively. Bright trions are formed directly through a phonon-assisted process upon optical excitation. Since the dark excitonic states lie energetically below the bright exciton, exciton-phonon scattering is highly efficient even at low temperatures, which accelerates the excitonic dephasing process as studied previously<sup>[58, 59]</sup>.

Since the studied  $\text{WSe}_2$  monolayer is n-type, the lower conduction band in both valleys has occupied states with spin orientation opposite to that of the valence band in the respective valley. Four possible conversion channels from bright to dark trions are proposed, as illustrated in Fig. 4. Upon excitation of the circularly-polarized light, either the bright singlet or triple trions could be formed, as diagrammed in Figs. 4(a) or 4(d). In the case of singlet trion that is formed entirely in the  $K$  valley as depicted in Fig. 4(a), the singlet trion could decay to a dark state via a phonon-assisted spin flip to the lower conduction band (Fig. 4(b)). Alternatively, the bright singlet trion could also decay to the lower energy dark trion through defect or phonon assisted momentum scattering to the  $K'$  valley (Fig. 4(c)). The dark trion can no longer relax radiatively, although its long valley relaxation recorded by Kerr rotation will persist because the absorption of the linearly-polarized probe will be affected by the population imbalance between  $K$  and  $K'$  valleys.

The triplet trion occupies both valleys, being composed of an optically excited electron and hole in the  $K$  valley, and an electron in the lower conduction band of the  $K'$  valley. In the case of bright triplet trion as shown in Fig. 4(d), a similar scattering processes could occur as that of the singlet trion. The optically excited electrons can undergo spin flip via phonon scattering to the lower conduction band within the same valley, as shown in Fig. 4(e), or undergo momentum scattering assisted by defects and phonons to the other valley, as depicted in Fig. 4(f). In both cases, the trion becomes dark, giving rise to a long-lived Kerr rotation response and a long valley spin lifetime. Although these four conversion channels from bright to dark trions can lead to long valley lifetime associated with dark trions, the intravalley spin-flip scattering as illustrated in Fig. 4(b) and Fig. 4(e) may have less chance to occur, especially at low temperatures. A previous study has suggested that the singlet trion decaying via spin-conserving intervalley scattering as depicted in Fig. 4(c) is most energetically favorable and is a symmetry-allowed channel<sup>[57, 60]</sup>. In addition, as we discussed earlier, the observed long spin lifetime  $\tau_{v3}$  should not originate from the resident electrons, whose spin lifetime cannot be so sensitive to the fine tuning of pump energy. Regardless of the peculiar dominant scattering channel, the efficient conversion from bright to dark trions that is facilitated via defect- and phonon-assisted intervalley scattering upon excitation is the most likely origin of the observed long valley lifetime  $\tau_{v3}$  in monolayer MBE- $\text{WSe}_2$ .

#### 4. Conclusion

In conclusion, the valley relaxation process for neutral excitons and trions in monolayer MBE- $\text{WSe}_2$  is investigated. A comparison study of TRKR with TRR reveals the long valley lifetime associated with dark trions in monolayer MBE- $\text{WSe}_2$ , which is evidenced by the excitation-energy-dependent TRKR measurements. Under photoexcitation at energies above the exciton resonance, the valley lifetime of trions is mainly determined by the rapid recombination and valley depolarization process of bright excitons or trions. A long trion spin lifetime up to 2.4 ns can be observed and is associated with the

formation of dark trion state when pumped at energy close to the trion resonance. The different valley dynamics in atomically thin TMDCs prepared by different growth methods require further exploration to achieve the robustness of the long-lived valley polarization.

#### Acknowledgements

This work was supported by the Strategic Priority Research Program of Chinese Academy of Sciences (No. XDB43000000).

#### References

- [1] Xiao D, Liu G B, Feng W X, et al. Coupled spin and valley physics in monolayers of  $\text{MoS}_2$  and other group-VI dichalcogenides. *Phys Rev Lett*, 2012, 108, 196802
- [2] Sallen G, Bouet L, Marie X, et al. Robust optical emission polarization in  $\text{MoS}_2$  monolayers through selective valley excitation. *Phys Rev B*, 2012, 86, 081301
- [3] Cao T, Wang G, Han W, et al. Valley-selective circular dichroism of monolayer molybdenum disulphide. *Nat Commun*, 2012, 3, 887
- [4] Mak K F, He K, Shan J, et al. Control of valley polarization in monolayer  $\text{MoS}_2$  by optical helicity. *Nat Nanotechnol*, 2012, 7, 494
- [5] Jones A M, Yu H, Ghimire N J, et al. Optical generation of excitonic valley coherence in monolayer  $\text{WSe}_2$ . *Nat Nanotechnol*, 2013, 8, 634
- [6] Xu X, Yao W, Xiao D, et al. Spin and pseudospins in layered transition metal dichalcogenides. *Nat Physics*, 2014, 10, 343
- [7] Shi H Y, Yan R S, Bertolazzi S, et al. Exciton dynamics in suspended monolayer and few-layer  $\text{MoS}_2$  2D crystals. *ACS Nano*, 2013, 7, 1072
- [8] Mai C, Barrette A, Yu Y F, et al. Many-body effects in valleytronics: Direct measurement of valley lifetimes in single-layer  $\text{MoS}_2$ . *Nano Lett*, 2014, 14, 202
- [9] Wang Q S, Ge S F, Li X, et al. Valley carrier dynamics in monolayer molybdenum disulfide from helicity-resolved ultrafast pump-probe spectroscopy. *ACS Nano*, 2013, 7, 11087
- [10] Cui Q N, Ceballos F, Kumar N, et al. Transient absorption microscopy of monolayer and bulk  $\text{WSe}_2$ . *ACS Nano*, 2014, 8, 2970
- [11] Wang G, Bouet L, Lagarde D, et al. Valley dynamics probed through charged and neutral exciton emission in monolayer  $\text{WSe}_2$ . *Phys Rev B*, 2014, 90, 075413
- [12] Lagarde D, Bouet L, Marie X, et al. Carrier and polarization dynamics in monolayer  $\text{MoS}_2$ . *Phys Rev Lett*, 2014, 112, 047401
- [13] Zhu C R, Zhang K, Glazov M, et al. Exciton valley dynamics probed by Kerr rotation in  $\text{WSe}_2$  monolayers. *Phys Rev B*, 2014, 90, 161302
- [14] dal Conte S, Bottegoni F, Pogna E A A, et al. Ultrafast valley relaxation dynamics in monolayer  $\text{MoS}_2$  probed by nonequilibrium optical techniques. *Phys Rev B*, 2015, 92, 235425
- [15] Yang L Y, Sinitsyn N A, Chen W B, et al. Long-lived nanosecond spin relaxation and spin coherence of electrons in monolayer  $\text{MoS}_2$  and  $\text{WS}_2$ . *Nat Phys*, 2015, 11, 830
- [16] Hsu W T, Chen Y L, Chen C H, et al. Optically initialized robust valley-polarized holes in monolayer  $\text{WSe}_2$ . *Nat Commun*, 2015, 6, 8963
- [17] Plechinger G, Nagler P, Arora A, et al. Trion fine structure and coupled spin-valley dynamics in monolayer tungsten disulfide. *Nat Commun*, 2016, 7, 12715
- [18] Song X L, Xie S E, Kang K, et al. Long-lived hole spin/valley polarization probed by kerr rotation in monolayer  $\text{WSe}_2$ . *Nano Lett*, 2016, 16, 5010

- [19] Dey P, Yang L Y, Robert C, et al. Gate-controlled spin-valley locking of resident carriers in WSe<sub>2</sub> monolayers. *Phys Rev Lett*, 2017, 119, 137401
- [20] Singh A, Tran K, Kolarczik M, et al. Long-lived valley polarization of intravalley trions in monolayer WSe<sub>2</sub>. *Phys Rev Lett*, 2016, 117, 257402
- [21] Volmer F, Pissinger S, Ersfeld M, et al. Intervalley dark trion states with spin lifetimes of 150 ns in WSe<sub>2</sub>. *Phys Rev B*, 2017, 95, 235408
- [22] McCormick E J, Newburger M J, Luo Y K, et al. Imaging spin dynamics in monolayer WS<sub>2</sub> by time-resolved Kerr rotation microscopy. *2D Mater*, 2017, 5, 011010
- [23] He K L, Kumar N, Zhao L, et al. Tightly bound excitons in monolayer WSe<sub>2</sub>. *Phys Rev Lett*, 2014, 113, 026803
- [24] Brem S, Ekman A, Christiansen D, et al. Phonon-assisted photoluminescence from indirect excitons in monolayers of transition-metal dichalcogenides. *Nano Lett*, 2020, 20, 2849
- [25] You Y, Zhang X X, Berkelbach T C, et al. Observation of biexcitons in monolayer WSe<sub>2</sub>. *Nat Phys*, 2015, 11, 477
- [26] van Tuan D, Scharf B, Wang Z F, et al. Probing many-body interactions in monolayer transition-metal dichalcogenides. *Phys Rev B*, 2019, 99, 085301
- [27] Feierabend M, Brem S, Ekman A, et al. Brightening of spin- and momentum-dark excitons in transition metal dichalcogenides. *2D Mater*, 2021, 8, 015013
- [28] Kusaba S, Watanabe K, Taniguchi T, et al. Role of dark exciton states in the relaxation dynamics of bright 1s excitons in monolayer WSe<sub>2</sub>. *Appl Phys Lett*, 2021, 119, 093101
- [29] Zhang X X, Cao T, Lu Z, et al. Magnetic brightening and control of dark excitons in monolayer WSe<sub>2</sub>. *Nat Nanotechnol*, 2017, 12, 883
- [30] Wang G, Robert C, Glazov M M, et al. In-plane propagation of light in transition metal dichalcogenide monolayers: Optical selection rules. *Phys Rev Lett*, 2017, 119, 047401
- [31] Ye J L, Niu B H, Li Y, et al. Exciton valley dynamics in monolayer Mo<sub>1-x</sub>W<sub>x</sub>Se<sub>2</sub> (x = 0, 0.5, 1). *Appl Phys Lett*, 2017, 111, 152106
- [32] Yan T F, Ye J L, Qiao X F, et al. Exciton valley dynamics in monolayer WSe<sub>2</sub> probed by the two-color ultrafast Kerr rotation. *Phys Chem Chem Phys*, 2017, 19, 3176
- [33] Arora A, Koperski M, Nogajewski K, et al. Excitonic resonances in thin films of WSe<sub>2</sub>: From monolayer to bulk material. *Nanoscale*, 2015, 7, 10421
- [34] Wang G, Chernikov A, Glazov M M, et al. *Colloquium*: Excitons in atomically thin transition metal dichalcogenides. *Rev Mod Phys*, 2018, 90, 021001
- [35] Adachi S. Luminescence spectroscopy of Cr<sup>3+</sup> in Al<sub>2</sub>O<sub>3</sub> polymorphs. *Opt Mater*, 2021, 114, 111000
- [36] Borghardt S, Tu J S, Winkler F, et al. Engineering of optical and electronic band gaps in transition metal dichalcogenide monolayers through external dielectric screening. *Phys Rev Mater*, 2017, 1, 054001
- [37] Cadiz F, Courtade E, Robert C, et al. Excitonic linewidth approaching the homogeneous limit in MoS<sub>2</sub> based van der Waals heterostructures. *Phys Rev X*, 2017, 7, 021026
- [38] Cho Y H, Gainer G H, Fischer A J, et al. S-shaped temperature-dependent emission shift and carrier dynamics in InGaN/GaN multiple quantum wells. *Appl Phys Lett*, 1998, 73, 1370
- [39] Yan T F, Qiao X F, Liu X N, et al. Photoluminescence properties and exciton dynamics in monolayer WSe<sub>2</sub>. *Appl Phys Lett*, 2014, 105, 101901
- [40] Courtade E, Semina M, Manca M, et al. Charged excitons in monolayer WSe<sub>2</sub>: Experiment and theory. *Phys Rev B*, 2017, 96, 085302
- [41] Förste J, Tepliakov N V, Kruchinin S Y, et al. Exciton g-factors in monolayer and bilayer WSe<sub>2</sub> from experiment and theory. *Nat Commun*, 2020, 11, 4539
- [42] Robert C, Lagarde D, Cadiz F, et al. Exciton radiative lifetime in transition metal dichalcogenide monolayers. *Phys Rev B*, 2016, 93, 205423
- [43] Ceballos F, Cui Q N, Bellus M Z, et al. Exciton formation in monolayer transition metal dichalcogenides. *Nanoscale*, 2016, 8, 11681
- [44] Yang M, Robert C, Lu Z G, et al. Exciton valley depolarization in monolayer transition-metal dichalcogenides. *Phys Rev B*, 2020, 101, 115307
- [45] Schmidt D, Godde T, Schmutzler J, et al. Exciton and trion dynamics in atomically thin MoSe<sub>2</sub> and WSe<sub>2</sub>: Effect of localization. *Phys Rev B*, 2016, 94, 165301
- [46] Yu T, Wu M W. Valley depolarization due to inter- and intra-valley electron-hole exchange interactions in monolayer MoS<sub>2</sub>. *Phys Rev B*, 2014, 89, 205303
- [47] Plechinger G, Korn T, Lupton J M. Valley-polarized exciton dynamics in exfoliated monolayer WSe<sub>2</sub>. *J Phys Chem C*, 2017, 121, 6409
- [48] Yu H, Liu G B, Gong P, et al. Dirac cones and Dirac saddle points of bright excitons in monolayer transition metal dichalcogenides. *Nat Commun*, 2014, 5, 3876
- [49] Singh A, Moody G, Wu S F, et al. Coherent electronic coupling in atomically thin MoSe<sub>2</sub>. *Phys Rev Lett*, 2014, 112, 216804
- [50] Schmidt R, Berghäuser G, Schneider R, et al. Ultrafast coulomb-induced intervalley coupling in atomically thin WS<sub>2</sub>. *Nano Lett*, 2016, 16, 2945
- [51] Pogna E A A, Marsili M, de Fazio D, et al. Photo-induced bandgap renormalization governs the ultrafast response of single-layer MoS<sub>2</sub>. *ACS Nano*, 2016, 10, 1182
- [52] Shinokita K, Wang X F, Miyauchi Y, et al. Ultrafast dynamics of bright and dark positive trions for valley polarization in monolayer WSe<sub>2</sub>. *Phys Rev B*, 2019, 99, 245307
- [53] Feldmann J, Peter G, Göbel E O, et al. Linewidth dependence of radiative exciton lifetimes in quantum wells. *Phys Rev Lett*, 1988, 60, 243
- [54] Sanvitto D, Hogg R A, Shields A J, et al. Rapid radiative decay of charged excitons. *Phys Rev B*, 2000, 62, R13294
- [55] Robert C, Park S, Cadiz F, et al. Spin/valley pumping of resident electrons in WSe<sub>2</sub> and WS<sub>2</sub> monolayers. *Nat Commun*, 2021, 12, 5455
- [56] Yan T F, Yang S Y, Li D, et al. Long valley relaxation time of free carriers in monolayer WSe<sub>2</sub>. *Phys Rev B*, 2017, 95, 241406
- [57] He M, Rivera P, van Tuan D, et al. Valley phonons and exciton complexes in a monolayer semiconductor. *Nat Commun*, 2020, 11, 618
- [58] Selig M, Berghäuser G, Raja A, et al. Excitonic linewidth and coherence lifetime in monolayer transition metal dichalcogenides. *Nat Commun*, 2016, 7, 13279
- [59] Song Y, Dery H. Transport theory of monolayer transition-metal dichalcogenides through symmetry. *Phys Rev Lett*, 2013, 111, 026601
- [60] Dery H, Song Y. Polarization analysis of excitons in monolayer and bilayer transition-metal dichalcogenides. *Phys Rev B*, 2015, 92, 125431



**Shengmin Hu** received his B.Sc. from North China Electric Power University in 2019. He is now a graduate student at University of Chinese Academy of Sciences under the supervision of Prof. Xinhui Zhang. His research focuses on the ultrafast valley pseudospin dynamics study in 2D semiconductors.



**Xinhui Zhang** is a professor at the Institute of Semiconductors (IOS), Chinese Academy of Sciences (CAS). She received her B.Sc. and M.Sc. degrees from Shaanxi Normal University, in 1991 and 1994 respectively, and PhD degree from the Institute of Physics, CAS in 1997. From 1997 to 2005, she worked as postdoc and research associate at Lund University (Sweden); College of William and Mary (USA); The University of Oklahoma (USA); and University of Moncton (Canada), respectively. Since 2006, she has worked as a professor at IOS, CAS. Her current research interests focus on the ultrafast spin dynamics in low-dimensional semiconductors and ferromagnet/semiconductor heterostructures.